

# Electrodeposition and characterization of CuInSe<sub>2</sub>/CdS multilayered thin films deposited on flexible substrate

V. SOARE, M. BURADA, D. MITRICA\*, V. BADILITA, F. STOICIU, C. P. LUNGU<sup>a</sup>, V. GHENESCU<sup>b</sup>,  
M. I. RUSU<sup>c,d</sup>, Ș. ANTOHE<sup>c</sup>

*National Research&Development Institute for nonferrous and Rare Metals – IMNR 102 Biruinței B-lvd, Postal code: 077145, Pantelimon, Ilfov, Romania*

<sup>a</sup>*National Institute for Laser, Plasma and Radiation Physics, Măgurele, Ilfov, Romania*

<sup>b</sup>*Space Science Institute, Măgurele, Ilfov, Romania*

<sup>c</sup>*University of Bucharest- Physics Faculty, Magurele, Ilfov, Romania*

<sup>d</sup>*National Institute of Research and Development for Optoelectronics, 409 Atomistilor Street, RO-077125 Măgurele, Ilfov, Romania*

Highly efficient multilayered thin films of Kapton/Ni/CIS/CdS/Al were obtained. Kapton is a plastic material with good flexibility, mechanical and high temperature resistance. A 1.5 micron layer of nickel was deposited on kapton material by TVA method. Single step co-deposition method was used to prepare the CIS layer. A subsequent 350 °C annealing was applied to improve CIS crystallinity and homogeneity. A CdS layer was deposited by single source thermal vacuum evaporation method. XRD and SEM-EDAX analyses confirmed a uniform and near to CIS stoichiometry composition. Ellipsometry revealed band gaps of 1.03 eV for CIS and 2.46eV for CdS, which confirm the literature data.

(Received November 1, 2010; accepted November 29, 2010)

*Keywords:* CIS, Thin films, Electrodeposition, Optoelectronic

## 1. Introduction

CIS(CdInSe<sub>2</sub>) thin films are some of the most efficient solar cell materials on the market. They represent the active layer of various solar cell systems, one of them being represented by Kapton/Ni/CIS/CdS/Al thin film multilayers.

Flexible substrates in highly efficient multilayered thin film solar cells eliminate weather induced deficiencies as thermal cracking, shock resistance and provide excellent electrical insulation. Kapton is a well known material used in electronic and electrical industry for its great properties of mechanical and high temperature resistance.

Single step co-deposition represents the most viable option among the yet known CIS thin layers preparation methods (molecular beam epitaxy-MBE [1], chemical vapor deposition-CVD [2], chemical bath deposition [3], evaporation [4] and RF sputtering [5]). Knowing that Cu, In and Se have different deposition potentials in the same electrolyte solution (i.e.  $\varepsilon_{Cu} = +0.342$  V,  $\varepsilon_{In} = -0.338$  V and  $\varepsilon_{Se} = +0.74$  V), improvements are needed to have all elements deposited in a single step electrolyses process [6]. In order to solve this problem complexing agents are added to the electrolyte solution. Gluconic acid as complexing agent brings closer the In and Cu deposition potentials by forming less stable complex compounds with Cu. Subsequent the thin film deposition method an annealing stage is applied to create a more uniform layer for wider optical absorption spectrum.

In this paper, a single step electrodeposition method was adopted to prepare CIS films. Kapton/Ni/CIS/CdS/Al multilayer fabrication implied different deposition methods. Resulted cell has become subject to SEM-EDAX, XRD and optoelectronic analyses.

## 2. Experimental

The experiments took place in a three electrode arrangement cell, containing a cathode, an anode and a reference electrode. The cell had capacity of 500 cm<sup>3</sup>. A saturated calomel electrode (SCE) was used as reference and the counter electrode was represented by a 30×30×0.5 mm platinum plate. The working electrode (cathode) was a Ni layered kapton foil with active area of 11 × 25 mm. The Ni layered kapton foil was attached to a solid non-conductive support material by a well conductive metal clip. The kapton foil was plated with metallic nickel by Thermionic Vacuum Arc method (TVA). The thickness of nickel film was aprox. 1 μm. The electrodeposition process was assisted by a Princeton Applied Research potentiostat / galvanostat model 263A and interfaced with data processing National Instruments specialized program Virtual PC 32. Electrolysis was conducted under heating (40°C) and continuous electrolyte stirring.

The experimental work has determined the influence of process parameters (electrolyte composition and current density) on morphology and composition of deposited thin film layer. The electrolyte compositions were represented by  $EI - 3 \times 10^{-3}$  [mole] CuSO<sub>4</sub>\*5H<sub>2</sub>O /  $3 \times 10^{-3}$  [mole]

In<sub>2</sub>(SO<sub>4</sub>)<sub>3</sub> / 10×10<sup>-3</sup> [mole] SeO<sub>2</sub> / 1 [mole] gluconic acid and E2 - 5×10<sup>-3</sup> [mole] CuSO<sub>4</sub>·5H<sub>2</sub>O / 10×10<sup>-3</sup> [mole] In<sub>2</sub>(SO<sub>4</sub>)<sub>3</sub> / 10\*10<sup>-3</sup> [mole] SeO<sub>2</sub> / 1 [mole] gluconic acid. Chemicals used in experiments were furnished by Sigma-Aldrich Germany, purity *p.a.* For each of the two different electrolyte concentrations, three different current densities were applied: 1.82 mA/cm<sup>2</sup>, 3.64 mA/cm<sup>2</sup> and 7.27 mA/cm<sup>2</sup>. The electrolyte pH was maintained at a desired value of 2.5 by adding NaOH and H<sub>2</sub>SO<sub>4</sub> solution. In order to remove dissolved oxygen, electrolyte solution was bubbled in advance for 5 minutes with nitrogen (purity 99.99% - Linde Gas Romania). Ni plated Kapton films were cleaned / degreased with acetone, washed with bidistilled water and dried by blowing argon gas unto the surface. The experimental work was performed at a voltage of 1 V, temperature 40 ° C and time period of 30 minutes. Electrolyte stirring was performed at a speed of 40 rpm. Obtained CIS thin films were rinsed with bidistilled water and dried with argon gas. To improve the crystallinity and composition distribution of the as-deposited films, the samples were heat treated in inert atmosphere at 350 °C for 1 h and later were cooled under Ar. After the heat treatment stage, samples were analyzed by XRD and SEM-EDAX to determine the physical-chemical characteristics of CIS layer.

CdS was deposited on to CIS layer by single source thermal vacuum evaporation method, from a quartz crucible at 700 °C, in vacuum atmosphere (2.2×10<sup>-4</sup> torr) to a substrate at 25 - 30 °C.

The multilayer thin film solar cell was completed by adding an aluminum hair comb type electrical contact.

### 3. Results and discussion

#### 3.1 Compositional analysis of CIS thin films

Chemical composition of single step electro-deposited layers was determined by EDAX characterization with a model S-2600N Hitachi scanning electron microscope with energy dispersive capability. The results obtained after the experimental stage showed better repartition of compositional elements in the deposited compound for the specimen corresponding to E2 concentration and 3,64 mA/cm<sup>2</sup> current density (Table 1 and Fig. 1).

The theoretical composition of CuInSe<sub>2</sub> compound is 25/25/50. After the single step electrodeposition process a close to stoichiometric composition was obtained (23/25/51). The lower percentage of Cu shows a good composition distribution of the film. Higher percentages of Cu determines usually better morphology but composition no nuniformities along the substrate [7]

Table 1. Optimal elementary composition obtained for deposited CuInSe<sub>2</sub> thin films.

Electrolyte	Current density (mA/cm <sup>2</sup> )	Cu	In	Se
		at. %	at. %	at. %
E2	3.64	23.72	25.24	51.04

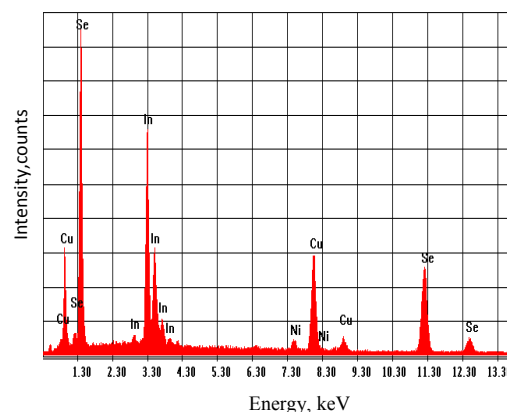


Fig. 1. EADX spectrum of the CIS thin film.

#### 3.2 Scanning electron microscopy analysis

SEM analysis of heat treated substrate (Fig. 2) was performed with a model S-2600N Hitachi scanning electron microscope. The SEM images indicate the presence of a polycrystalline structure, with large crystallites, relatively ordered, and separated by intercrystalline border areas of the same order of magnitude. The film morphology shows that Cu deficient samples (0.94 Cu/In) show a smooth, fine-grained, dense surface with large size crystallites. For areas of good uniformity and homogeneity, crystalline grain size was estimated in the range of 0,4-0,6 μm. Optical microscopy revealed average film thickness of aprox. 1.5-3 μm.

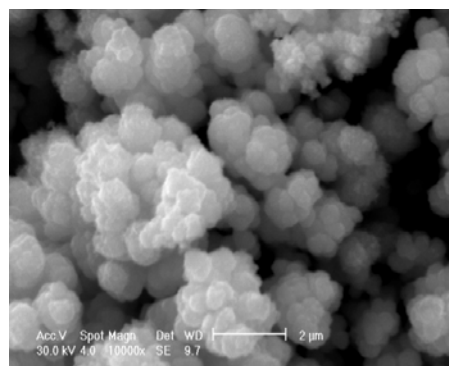
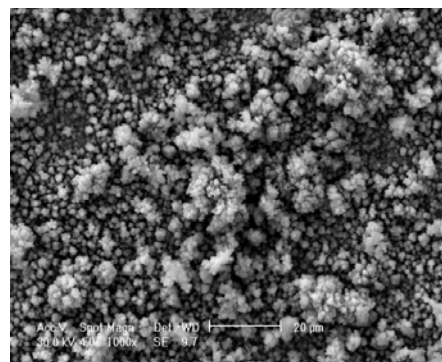


Fig. 2. SEM images of the CIS thin film.

### 3.3 X-ray diffraction analysis

Phase characterization was performed using a BRUKER D8 DISCOVER X-ray diffractometer connected to a data processing unit DIFFRAC<sup>plus</sup> BASIC Evaluation Package, version EVA12/2006 contained by DIFFRAC<sup>plus</sup> BASIC (Bruker AXS) software package and ICDD PDF-2 Release 2006. The CIS sample structure was studied with a Cu-K $\alpha_1$  ( $\lambda=1.5406\text{\AA}$ ) radiation wave length. In order to deliver a concentrated parallel beam, the diffractometer was equipped with a Goebel mirror and a V-groove monochromator, allowing the complete elimination of Cu-K $\alpha_2$ . Scanning step was set at  $\Delta(2\Theta) = 0.05\text{\AA}$ .

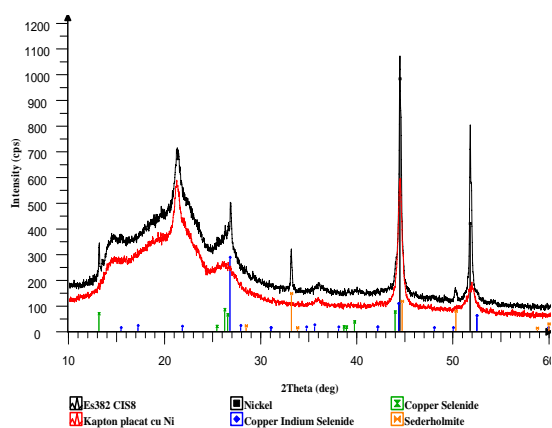


Fig. 3. X-ray analyses diagram of CIS thin film after annealing process.

X-ray interpretation for the co-deposited CIS films annealed at  $350\text{ }^\circ\text{C}$  confirms the presence of successive layers of Ni and CIS, containing primarily the active compound CuInSe $_2$ . Minor quantities of CuSe $_2$  and NiSe are showed (Fig. 3).

XRD patterns are showing the chalcopyrite structure (JCPDS 40-1487) as the major phase. A typical feature is that the samples exhibit a strong preferential orientation. Thus the most intense peak is situated at approximately  $26.58^\circ$ . The three main diffraction peaks due to (112), (204) and (312) planes correspond to CuInSe $_2$ . As seen in the diffractography of CuInSe $_2$  layer ( $2\theta=26.58^\circ$ ,  $44.18^\circ$  and  $52.34^\circ$ ) the peaks become higher and narrower due to the annealing process. The lattice constants for the chalcopyrite structure have been calculated to:  $a=5.782\text{ \AA}$  and  $c=11.61\text{ \AA}$ .

The CdS thin layer, analyzed with the same apparatus as the CIS layer, have a well defined wurtzite structure oriented by a (002) crystalline plane. The general appearance of the diffraction diagram suggests the existence of atomic plans packing defects along the axis (002) actually common in compact materials with crystalline structures.

### 3.4 Optoelectronic characterization

Ellipsometry measurements have determined the relationship between the incident photon energy and the extinction coefficient with respect to the refractive index of the specimen.

The material band gap was determined by extrapolating at  $\alpha = 0$  a chart of  $(\alpha h\nu)^2$  vs.  $h\nu$  (Fig. 4). The obtained value from experiments (1.03 eV) is consistent with results reported in the literature [8, 9].

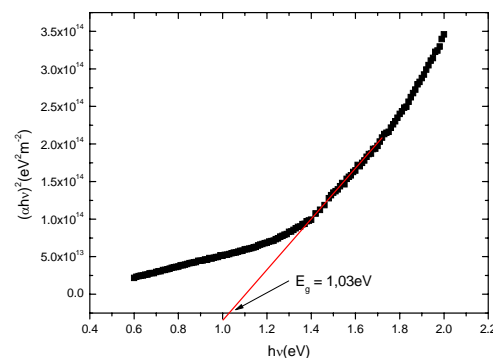


Fig. 4. CIS band gap calculation.

Transmission and absorption spectra for CdS deposited over the CIS layer were obtained using UV-VIS spectrophotometer Perkin Elmer Lambda 35. Measuring range used was from 190 nm to 1100 nm in air at room temperature. CIS thin films are direct band semiconductors, so the gap value can be determined from its optical absorption spectrum in the theoretical absorption region (Fig. 5).

By analyzing the absorption coefficient dependence on incident photon energy absorption in the specific area has been determined optical gap of CdS layers, deposited by thermal vacuum evaporation method (Fig. 6). The resulted value of 2.46 eV is in good agreement with the literature data [10].

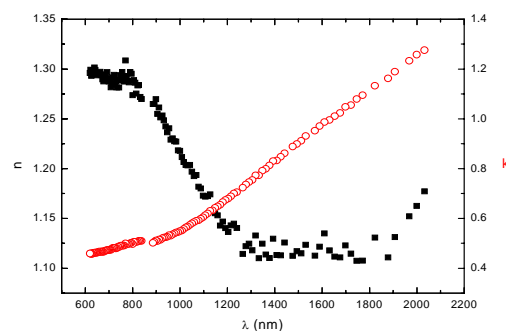


Fig. 5. Refraction coefficient -  $n$  and extinction coefficient -  $k$  for CIS in the NIR-VIS spectrum.

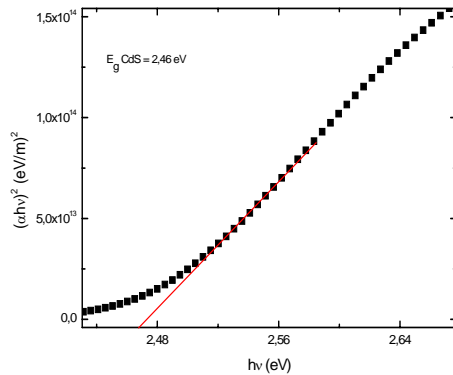


Fig. 6. CdS optical gap calculation.

Transmission measurements allowed for the determination of the thickness of CdS layer of 370 nm, using Swanepoel method [11].

The EQE action spectrum gives an indication of the spectral efficiency of CIS/CdS photovoltaic properties. For the sample whose spectrum of action is shown in Fig. 7, the spectral response contains essentially three bands: in the regions of 1000-1200 nm, 700-900 nm and 500-680 nm. The heterojunction CdS / CIS shows a gradual (less abrupt) transition between different wave length radiations. First photon absorption band is corresponding to the CIS absorption spectrum, second band (700-900 nm) is most likely attributed to the CdS/CIS interface, while the higher energy band (500-680 nm) is due to the photons absorbed in CdS layer. It is obvious that the heat treatment stage brought improvement results of both the interface CdS / CIS quality as well as chemical quality of the CIS layer.

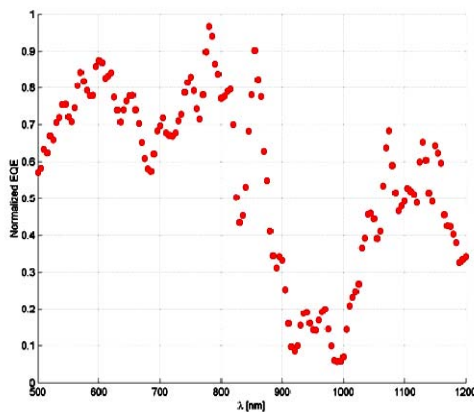


Fig. 7. EQE diagram for Kapton / Ni / CIS / CdS / Al, annealed at 350°C for 60 min.

#### 4. Conclusions

A Kapton/Ni/CIS/CdS/Al thin layer arrangement was fabricated by single step electrodeposition method in a three electrode cell. The cathode was represented by a flexible substrate of nickel plated plastic material (Kapton). The SEM-EDAX and XRD analyses of the CIS deposited layer showed a polycrystalline structure, with large and relatively ordered crystallites, of good composition distribution along the active area. A CdS layer was deposited on to CIS annealed surface by thermal vacuum evaporation method.

Optoelectronic characterization revealed good photon absorption properties of Kapton/Ni/CIS/CdS/Al thin layered cell. The annealing stage improved substantially the radiation absorption spectrum of the CIS material.

#### References

- [1] F. R. White, A. H. Clak, M. C. Gxaf, J. Appl. Phys. **50**, 544 (1979).
- [2] G. A. Mitchell, J. Sol. Energy Mater. and Sol. Cells, **57**, 1 (1996).
- [3] C. H. Huang, S. L. Sheng, W. N. Shafarman, C. H. Chang, E. S. Lambers, L. Rieth, J. W. Johnson, S. Kim, B. J. Stamberry, T. J. Anderson, P. H. Holloway, J. Sol Energy Mater. and Sol. Cells, **69**, 131 (2001).
- [4] J. M. Merino, M. Leon, F. Rueda, R. Diaz, J. Thin Solid Films, **22-27**, 361 (2000).
- [5] H. K. Song, S. G. Kim, H. J. Kim, S. K. Kim, K. W. Kang, J. C. Lee, K. H. Yoon, J. Sol. Energy Mater. Sol. Cells, **75**, 145 (2003).
- [6] C. J. Huang, T. H. Meen, M. Y. Lai, W. R. Chen, J. Sol. Energy Mater. Sol. Cells, **82**, 553 (2004).
- [7] R. E. Racheleau, J. D. Meakin, R. W. Birkmire, Proceedings of the 19th Institute of Electrical and Electronics Engineers Photovoltaic Specialists Conference (Institute of Electrical and Electronics Engineers, New York, 1988), p. 972
- [8] A. Gupta, S. Shrikata, S. Isomora, Solar Energy Materials and Solar Cells, **32**, 137(1994).
- [9] N. Kavcar, Solar Energy Materials and Solar Cells, **52**, 183 (1998).
- [10] B. Su, K. L. Choy Thin Solid Films, **359**, 144 (2000).
- [11] R. Swanepoel, Rev. Sci. Instrum., **16**, 1214 (1983).

\*Corresponding author: dmitrica@imnr.ro